Time-Dependent Adjoint Formulation for Metamaterial Optimization using Petrov-Galerkin Methods

Xueying Zhang, James C. Newman III, Weiyang Lin, and W. Kyle Anderson

Simcenter: Center of Excellence in Applied Computational Science and Engineering
University of Tennessee, Chattanooga, TN 37403, USA
Xueying-Zhang@mocs.utc.edu, James-Newman@utc.edu, Weiyang-Lin@mocs.utc.edu, Kyle-Anderson@utc.edu

Abstract ─ A time-dependent discrete adjoint algorithm for electromagnetic problems is presented. The governing equations are discretized with a semi-discrete Petrov-Galerkin method. Time advancement is accomplished using an implicit, second-order backward differentiation formula (BDF2). An all-dielectric metamaterial is proposed and gradient-based shape design optimization is conducted. Hicks-Henne functions are utilized for shape parameterization to ensure smooth surfaces, and linear elasticity employed to adapt interior mesh points to boundary modifications. The cost function used in the design optimization attempts to widen the bandwidth of the metamaterial over a desired frequency range. Optimization results demonstrate an increase of the full width at half maximum (FWHM) of reflection from 111 THz to 303 THz.

Index Terms ─ Adjoint-based sensitivity analysis, design optimization, finite element method, metamaterial, Petrov-Galerkin.

I. INTRODUCTION

In recent years, the Petrove-Galerkin (PG) method has become a popular approach in solving a wide range of convection-dominated problems, such as computational fluid dynamics and electromagnetics [1, 2]. The primary benefits of using PG methods arise from their suitability for efficient parallel computing and their high performance of efficiency over DG methods [1]. Since sensitivity analysis is required for gradient-based optimization, the PG method has been extended to provide sensitivity derivatives for both steady-state and time-dependent problems. To this end, a discrete adjoint approach for time-dependent acoustic problems is described in [3, 4] for a Petrov-Galerkin method.

Metamaterials [5] are artificially structured materials with sub-wavelength scale building blocks. The optical properties of metamaterials depend on the constituent materials and geometries of the building blocks. The ability to design such metamaterials opens the pathway for creating materials with designer optical properties. Over the past decade, metamaterials have shown the ability of controlling light propagation [6], absorption and emission [7, 8]. The rapid development of metamaterial research has lead to many scientific breakthroughs such as negative refraction, invisible cloaking, and ultra-compact optical elements [5-9].

In this paper, the research described in [3, 10] is extended for optimization of metamaterials at optical frequencies. A time-dependent discrete adjoint method is employed to obtain sensitivity derivatives. An all-dielectric metamaterial is proposed and optimization is conducted. To follow, the governing equations and discretization method, the adjoint-based sensitivity analysis and shape optimization algorithm, and numerical results are presented.

II. GOVERNING EQUATIONS AND DISCRETIZATION METHOD

The governing equations considered are the two-dimensional source-free Maxwell's equations, which can be written in the conservative form:

$$\frac{\partial q(x,t)}{\partial t} + \frac{\partial F(q(x,t))}{\partial x} + \frac{\partial G(q(x,t))}{\partial y} = 0, \qquad (1)$$

where q, F and G are given by:

$$q = \{D_x, D_y, B_z\}^T,$$
$$F = \{0, B_z/\mu, D_y/\varepsilon\}^T, G$$
$$= \{-B_z/\mu, 0, -D_x/\varepsilon\}^T, \qquad (2)$$

or

$$q = \{B_x, B_y, D_z\}^T,$$
$$F = \{0, -D_z/\varepsilon, -B_y/\mu\}^T, G$$
$$= \{D_z/\varepsilon, 0, B_x/\mu\}^T, \qquad (3)$$

for a transverse-electric (TE) mode or a transverse-magnetic (TM) mode, respectively. In the equations above, μ and ε represent the relative permeability and permittivity, respectively. These parameters are assumed to be constants in the current work.

The Petrov-Galerkin discretization begins by formulating a weighted-integral statement of the governing equations by multiplying Eq. (1) by a set of weighting functions, and integrating within each element, as:

$$\int_{\Omega_k}[\phi]\left(\frac{\partial q}{\partial t} + \frac{\partial F}{\partial x} + \frac{\partial G}{\partial y}\right)d\Omega_k = 0, \qquad (4)$$

where ϕ is a weighting function defined by the Streamline Upwind/Petrov-Galerkn (SUPG) method given by:

$$[\phi] = N[I] + \left(\frac{\partial N}{\partial x}[A] + \frac{\partial N}{\partial y}[B]\right)[\tau] \qquad (5)$$
$$= N[I] + [P],$$

where $[\tau]$ represents the stabilization matrix and can be obtained using the following definitions:

$$[\tau]^{-1} = \sum_{k=1}^{n}\left|\frac{\partial N_k}{\partial x}[A] + \frac{\partial N_k}{\partial y}[B]\right|, \qquad (6)$$

$$\left|\frac{\partial N_k}{\partial x}[A] + \frac{\partial N_k}{\partial y}[B]\right| = [T][|\Lambda|][T]^{-1}, \qquad (7)$$

where $[T]$ and $[\Lambda]$ are the right eigenvectors and eigenvalues of the matrix on the left hand side of Eq. (7) respectively, and $[T]^{-1}$ represents the inverse of $[T]$.

Integrating Eq. (4) by parts, the weak formulation of the problem for each elementcan be written as:

$$\int_{\Omega_k} N_i\frac{\partial \boldsymbol{q_p}}{\partial t}d\Omega_k - \int_{\Omega_k}\left[\frac{\partial N_i}{\partial x}F(\boldsymbol{q_p}) + \right.$$
$$\left.\frac{\partial N_i}{\partial y}G(\boldsymbol{q_p})\right]d\Omega_k + \int_{\Omega_k}[P]\left[\frac{\partial \boldsymbol{q_p}}{\partial t} + \frac{\partial F(\boldsymbol{q_p})}{\partial x} + \right. \qquad (8)$$
$$\left.\frac{\partial G(\boldsymbol{q_p})}{\partial y}\right]d\Omega_k + \int_{\Gamma_k}N_i H(\boldsymbol{q_p^+},\boldsymbol{q_p^-},\boldsymbol{n})dS = 0,$$

where the solution is approximated as $q_p = \sum_{i=1}^{M}\tilde{q}_{p_i}N_i(x)$. In Eq. (8), $H(q_p^+, q_p^-, n)$ represents the flux on the element boundaries, which is determined from the data on either side of the interface using a Riemann solver described in [1]. Equation (8) can be written as an ordinary differential equation in time, which is integrated using an implicit, second-order backward difference formula (BDF2).

III. ADJOINT-BASED UNSTEADY SHAPE OPTIMIZATION

In gradient-based optimization, sensitivity derivatives of the objective function are utilized to construct an appropriate search direction for improving the design. For the direct approach a linear system is formed and solved for each design variable. Numerical evaluation, such as central finite-difference, requires two high converged solutions for each design variable. When the number of design variables is greater than the number of objective functions, adjoint-based sensitivity analysis is the most efficient option for obtaining these derivatives. The number of linear systems requiring solution is equal to the number of objective functions.

A. Design variables and shape parametrization

During a design cycle, the geometry is modified through surface node displacements according to a defined parameterization. The specific method will dictate the set of geometric design variables. A number of surface parameterization methods have been utilized for this purpose in the literature, such as Bezier, B-spline, Hicks-Henne functions, basis vectors, free-

form deformation, etc. In this paper, the Hicks-Henne sine bump function is utilized to ensure smooth surface shape, given by:

$$b_i(x_{si},\beta_m) = \beta_m sin^4\left(\pi x_{si}^{\ln(0.5)/\ln(x_{sm})}\right), \qquad (9)$$

where the design variables are set to be the magnitudes of the bump functions $\boldsymbol{\beta} = \{\beta_m, m = 1,\cdots,N_d\}$, where N_d represents the total number of design variables. In Eq. (9), b_i represents the surface node displacement at x_{si} due to the displacement of the surface node at x_{sm}, and β_m denotes the mth component of the design variables associated with the surface node at x_{sm}. The modified surface coordinates are computed by:

$$x_{si}^{new} = x_{si}^{old} + \sum_{m=1}^{N_d} b_i(x_{si},\beta_m). \qquad (10)$$

As the surface mesh deformation is obtained, the interior mesh points are deformed using linear elasticity to prevent the generation of overlapping elements. This system of equations may be expressed as $[K]\Delta x = \Delta x_s$, where $[K]$ represents the stiffness matrix as found in solid mechanics applications.

For gradient-based optimization the function I refers to a scalar-valued objective function used for minimization. A general formulation for the objective function is expressed in terms of the design variables as $I = I\left(X(\boldsymbol{\beta}),\tilde{q}(X(\boldsymbol{\beta}))\right)$, where $\tilde{q}$ represents the computed unsteady solution, X represents the computational mesh and $\boldsymbol{\beta}$ represents the set of design variables, which control the modification of the surface geometry.

B. Adjoint-base sensitivity calculation

The unsteady residual for time step n can be expressed as:

$$R^n(\boldsymbol{\beta},X,\tilde{\boldsymbol{q}}^n,\tilde{\boldsymbol{q}}^{n-1},\tilde{\boldsymbol{q}}^{n-2}) = 0. \qquad (11)$$

The sensitivity derivative can be computed using a forward mode direct differentiation by examining the function dependencies of the objective function. The total differential of I with respect to β can be expressed as:

$$\frac{dI}{d\beta} = \frac{\partial I}{\partial X}\frac{\partial X}{\partial \beta} - \sum_{n=1}^{ncyc}\frac{\partial I}{\partial q^n}\left[\frac{\partial R^n}{\partial q^n}\right]^{-1}\left(\frac{\partial R^n}{\partial X}\frac{\partial X}{\partial \beta} + \right.$$
$$\left.\frac{\partial R^n}{\partial q^{n-1}}\frac{\partial q^{n-1}}{\partial \beta} + \frac{\partial R^n}{\partial q^{n-2}}\frac{\partial q^{n-2}}{\partial \beta}\right). \qquad (12)$$

The adjoint method eliminates the computational overhead caused by repetitive calculations of the solution sensitivities by transposing the inverse of the Jacobian matrix. While a detailed derivation of the procedure is given in [3], the total differential of the objective function may be expressed in terms of the adjoint vector as:

$$\frac{dI}{d\beta} = \frac{\partial I}{\partial X}\frac{\partial X}{\partial \beta} + \sum_{n=1}^{ncyc}\left([\lambda_q^n]^T\left(\frac{\partial R^n}{\partial X}\frac{\partial X}{\partial \beta}\right)\right), \qquad (13)$$

where

$$\lambda_q^n = -\left[\frac{\partial R^n}{\partial q^n}\right]^{-T}\left(\left[\frac{\partial I}{\partial q^n}\right]^T + [\psi_1^{n+1}]^T + \right.$$
$$\left.[\psi_2^{n+2}]^T\right), \qquad (14)$$

$$\psi_1^n = \left[\frac{\partial R^n}{\partial q^{n-1}}\right]^T \lambda_q^n, \quad \psi_2^n = \left[\frac{\partial R^n}{\partial q^{n-2}}\right]^T \lambda_q^n, \qquad (15)$$

are the adjoint variables.

C. Shape optimization algorithm

Once the sensitivity derivatives of the objective function are evaluated, they are utilized to predict an appropriate search direction. The basic algorithm can be written as:

Algorithm. A discrete adjoint formulation for time-dependent sensitivity derivatives:

(1) Set ψ_1^{n+1}, ψ_2^{n+1}, ψ_2^{n+2} to be zero. Set n to be ncyc.
(2) Solve Eq. (14) for the adjoint variable.
(3) Set the sensitivity derivatives by:

$$\frac{dI}{d\beta} = \frac{dI}{d\beta} + \frac{\partial I}{\partial X}\frac{\partial X}{\partial \beta} + \left[\lambda_q^n\right]^T \left(\frac{\partial R^n}{\partial X}\frac{\partial X}{\partial \beta}\right). \qquad (16)$$

(4) Set $n = n - 1$.
(5) Set $\psi_2^{n+2} = \psi_2^{n+1}$, solve Eq. (15) for ψ_1^{n+1} and ψ_2^{n+1}.
(6) If $n = 1$, stop; otherwise go to step 2.

IV. NUMERICAL RESULTS

A. All-dielectric metamaterial and objective function

All-dielectric metamaterials offer a potential low-loss alternative to plasmonic metamaterials at optical frequencies [11]. In the current work, an all-dielectric metamaterial made of silicon on SiO$_2$ substrate is proposed as the initial design model. Figures 1 (a-b) illustrate the schematic of metamaterial unit cell and array. The silicon resonators with dimension of W = 200 nm and H = 100 nm are placed on top of a SiO$_2$ substrate (regarded infinite) with periodicity of P = 300nm. As shown the Fig. 1 (a), the metamaterial is illuminated with polarized light. The electric field is polarized along the x-direction and the magnetic field along the y-direction with wave vector k in z-direction. In this case, the light transmits from the air to the SiO$_2$ through the silicon resonators.

The metamaterial proposed above is modeled and simulated by an in-house code developed at the Simcenter. The results of reflection over frequency range of 350-650 THz are shown in Fig. 1 (c), with full width at half maximum (FWHM) of 111 THz (479~590 THz) in reflection. For comparative purposes, the current results are shown with those from the commercial software ANSYS© HFSS [12]. The reflection indicates that the metamaterial has the maximum reflection at 516 THz. The electric field distribution at 516 THz, depicted in Fig. 1 (d), clearly illustrates this reflection.

The objective of the current design optimization is to widen the bandwidth of the metamaterial. Accordingly, an objective function is proposed as:

$$I = \int_{f1}^{f2}(1 - Reflection)^2 \, df, \qquad (17)$$

where f_1 and f_2 represent the lower and upper bound of the desired frequency range.

B. Optimization results

In the current research the DAKOTA toolkit [13] was utilized. DAKOTA's optimization capabilities include a wide variety of optimization methods, and an interface to link with third-party routines. The optimization is performed using a quasi-Newton method (DAKOTA's OPT++ library [14]) based on the Broyden-Fletcher-Goldfard-Shanno (BFGS) variable-metric algorithm, and the line searching approach of More and Thuente [15].

Utilizing the objective function given in Eq. (17), with $f_1 = 300 \, THz$ and $f_2 = 700 \, THz$, the optimization was performed using different numbers of design variables. Increasing the number of design variables allows for greater geometric flexibility. Figure 2 illustrates the optimization results with 1, 3, and 9 design variables. As seen in Fig. 2 (a), at 426 THz no reflection can be observed from the electric field distribution for the initial model, while high reflection can be observed for the optimized geometries in Figs. 2 (b)-(d) using different number of design variables.

As shown in Fig. 3, the FWHM of reflection for the all-dielectric metamaterial increases from 111 THz to 277 THz, 285 THz, and 303 THz with 1, 3, and 9 design variables, respectively. For the optimized result with 9 design variables, the FWHM of reflection ranges from 376 to 679 THz. As shown in Fig. 4, the electric field distributions at 404 THz, 505 THz and 620 THz are simulated to demonstrate the high reflection property of the optimized metamaterial over the wide frequency range.
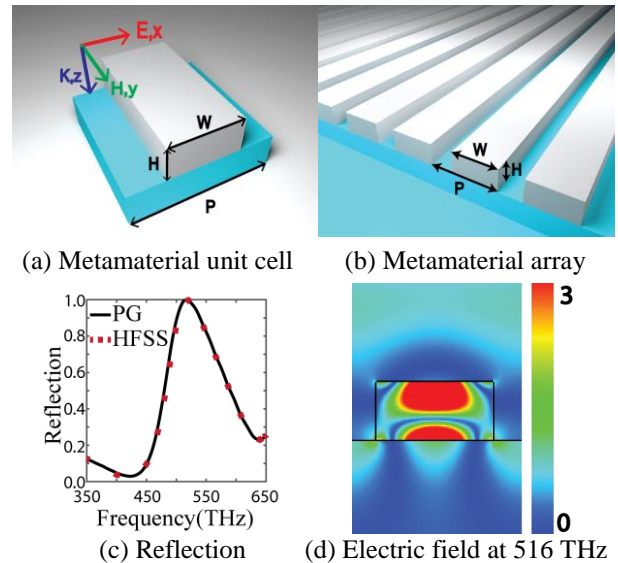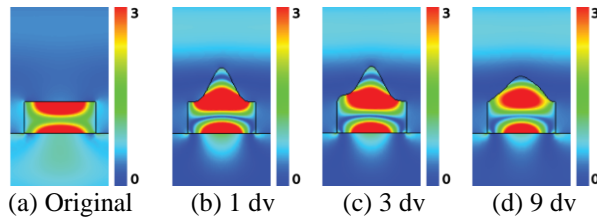

(a) Metamaterial unit cell (b) Metamaterial array

(c) Reflection (d) Electric field at 516 THz

Fig. 1. Proposed initial metamaterial model.

(a) Original   (b) 1 dv   (c) 3 dv   (d) 9 dv

Fig. 2. Electric field distribution at 426 THz.
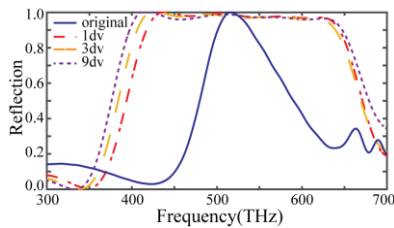
Fig. 3. Comparison of reflection over 300-700 THz.

(a) 404 THz   (b) 505 THz   (c) 620 THz
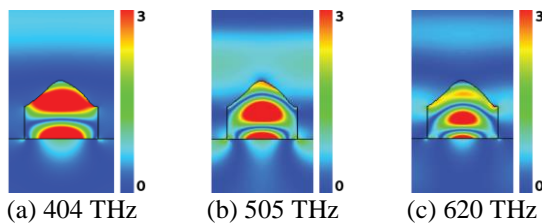
Fig. 4. Electric field distribution of model with 9dv.

V. CONCLUSION

This paper presents an unsteady discrete adjoint approach for performing sensitivity analysis as required by gradient-based optimization algorithms. The simulations are performed by discretizing the source-free Maxwell equations using a Petrov-Galerkin finite-element method. Temporal accuracy is achieved with an implicit, second-order backward differentiation formula (BDF2). Electromagnetic shape optimization is conducted on an all-dielectric metamaterial working at optical frequencies, and considers multiple numbers of design variables. Furthermore, utilizing the current shape optimization procedure the FWHM of reflection was increased from 111 THz to 303 THz.

ACKNOWLEDGMENT

REFERENCES

[1] W. K. Anderson, L. Wang, S. Kapadia, C. Tanis, and B. Hilbert, "Petrov-Galerkin and discontinuous-Galerkin methods for time-domain and frequency-domain electromagnetic simulations," *J. Comput. Phys.*, vol. 230, pp. 8360-8385, 2011.

[2] W. K. Anderson, L. Wang, J. C. Newman III, and S. Kapadia, "Extension of the Petrov-Galerkin time-domain algorithm for dispersive media," *IEEE Microw. Wirel. Compon. Lett.*, vol. 23, no. 5, pp. 234-236, 2013.

[3] W. Lin, W. K. Anderson, J. C. Newman III, and X. Zhang, "Shape optimization of two-dimensional acoustic metamaterials and phononic crystals with a time-dependent adjoint formulation," *AIAA Paper 2016-3830*, 2016.

[4] W. Lin, J. C. Newman III, W. K. Anderson, and X. Zhang, "Broadband shape and topology optimization of acoustic metamaterials and phononic crystals," *AIAA Paper* 2016-3216, 2016.

[5] R. A. Shelby, D. R. Smith, and S. Schultz, "Experimental verification of a negative index of refraction," *Science*, vol. 292, pp. 77-79, 2001.

[6] J. Valentine, S. Zhang, T. Zentgraf, E. Ulin-Avila, D. A. Genov, G. Bartal, and X. Zhang, "Three-dimensional optical metamaterial with a negative refractive index," *Nature*, vol. 455, no. 7211, pp. 376-379, 2008.

[7] W. Li and J. Valentine, "Metamaterial perfect absorber based hot electron photodetection," *Nano Lett.*, vol. 14, no. 6, pp. 3510-3514, 2014.

[8] X. Liu, T. Tyler, T. Starr, A. F. Starr, N. M. Jokerst, and W. J. Padilla, "Taming the blackbody with infrared metamaterials as selective thermal emitters," *Phys. Rev. Lett.*, vol. 107, no. 4:045901, 2011.

[9] W. Li, Z. J. Coppens, L. V. Besteiro, W. Wang, A. O. Govorov, and J. Valentine, "Circularly polarized light detection with hot electrons in chiral plasmonic metamaterials," *Nat. Commun.*, vol. 6:8379, 2015.

[10] L. Wang and W. K. Anderson, "Adjoint-based shape optimization for electromagnetic problems using discontinuous Galerkin methods," *AIAA J.*, vol. 49, no. 6, pp. 1302-1305, 2011.

[11] P. Moitra, B. A. Slovick, W. Li, I. I. Kravchencko, D. P. Briggs, S. Krishnamurthy, and J. Valentine, "Large-scale all-dielectric metamaterial perfect reflectors," *ACS Photonics*, vol. 2, no. 2, pp. 692-698, 2015.

[12] Ansoft High Frequency Structure Simulation (HFSS), ver. 12.0, Ansoft Corporation, Pittsburgh, PA, 2009.

[13] B. M. Adams, L. E. Bauman, W. J. Bohnhoff, K. R. Dalbey, M. S. Ebeida, J. P. Eddy, M. S. Eldred, P. D. Hough, K. T. Hu, J. D. Jakeman, L. P. Swiler and D. M. Vigil, "DAKOTA: version 5.2 user's manual," *Sandia Tech. Rep.*, SAND2010-2183, 2009.

[14] J. C. Meza, R. A. Oliva, P. D. Hough, and P. J. Williams, "OPT++: An object oriented toolkit for nonlinear optimization," *ACM Trans. Math. Software*, vol. 33, no. 2, pp. 126-136, 2007.

[15] J. J. More and D. J. Thuente, "Line search algorithms with guaranteed sufficient decrease," *ACM Trans. Math. Software*, vol. 20, pp. 286-307, 1994.